

Supplementary Information for "Potassium Clearance in Optic Nerve: a Multidomain Model"

Shanfeng Xiao ^{*} Huaxiong Huang [†] Robert Eisenberg [‡] Zilong Song [§]
 Shixin Xu [¶]

1 Mathematical Model Details

1.1 Ion Transport

The conservation of ion species implies the following system of partial differential equations to describe the dynamics of ions in each region, for $i = \text{Na}^+, \text{K}^+, \text{Cl}^-$ in domain Ω_{OP}

$$\frac{\partial \eta_{ax} C_{ax}^i}{\partial t} + \mathcal{M}_{ax,ex} J_{ax,ex}^i + \frac{\partial}{\partial z} (\eta_{ax} j_{ax,z}^i) = 0, \quad (1a)$$

$$\frac{\partial \eta_{gl} C_{gl}^i}{\partial t} + \mathcal{M}_{gl,ex} J_{gl,ex}^i + \mathcal{M}_{gl,pa} J_{gl,pa}^i + \mathcal{M}_{gl,pv} J_{gl,pv}^i + \mathcal{M}_{gl,pc} J_{gl,pc}^i + \nabla \cdot (\eta_{gl} \mathbf{j}_{gl}^i) = 0, \quad (1b)$$

$$\frac{\partial \eta_{pa} C_{pa}^i}{\partial t} + \mathcal{M}_{pa,ex} J_{pa,ex}^i - \mathcal{M}_{gl,pa} J_{gl,pa}^{m,i} + \mathcal{M}_{pa,pc} J_{pa,pc}^i + \nabla \cdot (\eta_{pa} \mathbf{j}_{pa}^i) = 0, \quad (1c)$$

$$\frac{\partial \eta_{pv} C_{pv}^i}{\partial t} + \mathcal{M}_{pv,ex} J_{pv,ex}^i - \mathcal{M}_{gl,pv} J_{gl,pv}^{m,i} - \mathcal{M}_{pc,pv} J_{pc,pv}^i + \nabla \cdot (\eta_{pv} \mathbf{j}_{pv}^i) = 0, \quad (1d)$$

$$\frac{\partial \eta_{pc} C_{pc}^i}{\partial t} + \mathcal{M}_{pc,ex} J_{pc,ex}^i - \mathcal{M}_{gl,pc} J_{gl,pc}^i - \mathcal{M}_{pa,pc} J_{pa,pc}^i + \mathcal{M}_{pc,pv} J_{pc,pv}^i + \nabla \cdot (\eta_{pc} \mathbf{j}_{pc}^i) = 0, \quad (1e)$$

$$\frac{\partial \eta_{ex} C_{ex}^i}{\partial t} - \sum_{k=ax,gl,pa,pv,pc} \mathcal{M}_{k,ex} J_{k,ex}^i + \nabla \cdot (\eta_{ex} \mathbf{j}_{ex}^i) = 0, \quad (1f)$$

and in the Ω_{SAS} region,

$$\frac{\partial C_{csf}^i}{\partial t} + \nabla \cdot (\mathbf{j}_{csf}^i) = 0. \quad (2)$$

Transmembrane Ion Flux The transmembrane ion flux $J_{l,k}^i$ ($l, k = ax, ex; gl, ex; gl, pa; gl, pv; gl, pc$) consists of an active ion pump source $J_{l,k}^{p,i}$ and passive ion channel source $J_{l,k}^{c,i}$,

$$J_{l,k}^i = J_{l,k}^{p,i} + J_{l,k}^{c,i}; \quad i = \text{Na}^+, \text{K}^+, \text{Cl}^-.$$

Due to the gaps between astrocytes endfeet [1], the transmembrane ion flux $J_{l,k}^i$ between perivascular spaces and ECS ($l, k = pa, ex; pv, ex; pc, ex$) consists of direct transportation with fluid $C_{up,wind}^i U_{l,k}$ and passive ion channel source $J_{l,k}^{c,i}$,

^{*}School of Mathematical Sciences, Soochow University, 1 Shi-Zi Street, Suzhou 215006, Jiangsu Province, China

[†]Zu Chongzhi Center for Mathematics and Computational Sciences, Duke Kunshan University, 8 Duke Ave, Kunshan, China; Guangdong Provincial Key Laboratory of Interdisciplinary Research and Application for Data Science, BNU-HKBU United International College, Zhuhai 519088, China; Department of Mathematics and Statistics York University, Toronto, ON M3J 1P3, Canada

[‡]Department of Applied Mathematics, Illinois Institute of Technology, Chicago, IL 60616, USA

[§]Math and Statistics Department, Utah State University, Old Main Hill, Logan, UT 84322, USA

[¶]Zu Chongzhi Center for Mathematics and Computational Sciences, Duke Kunshan University, 8 Duke Ave, Kunshan, China

$$J_{l,k}^i = C_{up,wind}^i U_{l,k} + J_{l,k}^{c,i}; \quad i = \text{Na}^+, \text{K}^+, \text{Cl}^-.$$

Because of the direct connection, the communication ion flux $J_{l,k}^i$ between perivascular spaces only depends on transportation with fluid $C_{up,wind}^i U_{l,k}$,

$$J_{l,k}^i = C_{up,wind}^i U_{l,k}; \quad i = \text{Na}^+, \text{K}^+, \text{Cl}^-.$$

On the glial cell membranes, $J_{gl,k}^{c,i}$ is defined as

$$J_{gl,k}^{c,i} = \frac{g_{gl}^i}{z^i e} (\phi_{gl} - \phi_k - E_{gl,k}^i), \quad i = \text{Na}^+, \text{K}^+, \text{Cl}^-, \quad k = \text{ex}, \text{pa}, \text{pv}, \text{pc}, \quad (3)$$

where $E_{gl,k}^i$ is the Nernst potential that describes the gradient of chemical potential in electrical units

$$E_{gl,k}^i = \frac{k_B T}{e z^i} \log \left(\frac{C_k^i}{C_{gl}^i} \right), \quad k = \text{ex}, \text{pa}, \text{pv}, \text{pc}$$

and the conductance g_{gl}^i for the i th ion species on the glial membrane is a fixed constant, independent of voltage and time.

On the axon's membrane, $J_{ax,ex}^{c,i}$ is defined as

$$J_{ax,ex}^{c,i} = \frac{g_{ax}^i}{z^i e} (\phi_{ax} - \phi_{ex} - E_{ax}^i), \quad i = \text{Na}^+, \text{K}^+, \text{Cl}^-, \quad (4)$$

where the conductances of Na^+ and K^+ are modeled using the Hodgkin-Huxley model [2, 3]

$$g_{ax}^{Na} = \bar{g}^{Na} m^3 h + g_{leak}^{Na}, \quad g_{ax}^K = \bar{g}^K n^4 + g_{leak}^K, \quad g_{ax}^{Cl} = g_{leak}^{Cl}.$$

$$\begin{cases} \frac{dn}{dt} = \alpha_n(1-n) - \beta_n n, \\ \frac{dm}{dt} = \alpha_m(1-m) - \beta_m m, \\ \frac{dh}{dt} = \alpha_h(1-h) - \beta_h h, \end{cases} \quad (5)$$

where n is the open probability of K^+ channel, m is the open probability of the Na^+ activation gate, and h is the open probability of the Na^+ inactivation gate. α_i and β_i for $i = n, m, h$ are active and inactive rates of different gate.

For the active ion pump source $J_{l,k}^{p,i}$, the only pump we consider is the Na/K active transporter. We are more than aware that other active transport systems can and likely do move ions and fluid in this system. They will be included as experimental information becomes available. In the case of the Na/K pump $J_{l,k}^{p,i}$, ($l, k = ax, ex; gl, pa; gl, pv; gl, pc$), the strength of the pump depends on the concentration in the intracellular and extracellular spaces [2, 4], such that

$$J_{l,k}^{p,Na} = \frac{3I_l}{e}, \quad J_{l,k}^{p,K} = -\frac{2I_l}{e}, \quad J_{l,k}^{p,Cl} = 0, \quad l = ax, gl, \quad (6)$$

where

$$I_l = I_{l,1} \left(\frac{C_l^{Na}}{C_l^{Na} + K_{Na1}} \right)^3 \left(\frac{C_{ex}^K}{C_{ex}^K + K_{K1}} \right)^2 + I_{l,2} \left(\frac{C_l^{Na}}{C_l^{Na} + K_{Na2}} \right)^3 \left(\frac{C_{ex}^K}{C_{ex}^K + K_{K2}} \right)^2,$$

$I_{l,1}$ and $I_{l,2}$ are related to α_1 - and α_2 - isoform of Na/K pump.

Remark 1 *In this study, we use a simplified representation of K^+ channels as a starting point, which was used in the previous work [5], and calibrated with the experiment results [6]. We acknowledge that this is an oversimplification, as different types of K^+ channels exhibit varying properties and are likely distributed in specific locations with different densities for biological reasons. When experimental data become available, these properties can be integrated into the model. The model is designed to be flexible, allowing for the incorporation of detailed channel characteristics without placing an undue burden on computational resources or programming complexity.*

Ion Flux inside Compartment The definitions of ion flux in each domain are as follows, for $i = \text{Na}^+, \text{K}^+, \text{Cl}^-$,

$$\mathbf{j}_l^i = C_l^i \mathbf{u}_l - D_l^i \nabla \left(\nabla C_l^i + \frac{z^i e}{k_B T} C_l^i \nabla \phi_l \right), \quad l = gl, ex, pa, pv, pc, \quad (7a)$$

$$j_{ax,z}^i = C_{ax}^i u_{ax}^z - D_{ax}^i \left(\frac{\partial C_{ax}^i}{\partial z} + \frac{z^i e}{k_B T} C_{ax}^i \frac{\partial \phi_{ax}}{\partial z} \right). \quad (7b)$$

Boundary Conditions For the axon and glial compartment boundary condition, we use the membrane boundary conditions at location $\Gamma_2 \cup \Gamma_6$. The homogeneous Neumann boundary condition on the Γ_1 and a non-flux boundary condition is used on the pia mater Γ_7 for the glial compartment.

$$\begin{cases} \nabla C_{gl}^i \cdot \hat{\mathbf{n}}_r = 0, & \text{on } \Gamma_1, \\ \nabla C_{ax}^i \cdot \hat{\mathbf{n}}_z = \lambda_{ax,left}(C_{ax}^i - C_{ax}^{i,re}), \quad \nabla C_{gl}^i \cdot \hat{\mathbf{n}}_z = \lambda_{gl,left}(C_{gl}^i - C_{gl}^{i,re}), & \text{on } \Gamma_2, \\ \nabla C_{ax}^i \cdot \hat{\mathbf{n}}_z = \lambda_{ax,right}(C_{ax}^i - C_{ax}^{i,re}), \quad \nabla C_{gl}^i \cdot \hat{\mathbf{n}}_z = \lambda_{gl,right}(C_{gl}^i - C_{gl}^{i,re}), & \text{on } \Gamma_6, \\ \mathbf{j}_{gl}^i \cdot \hat{\mathbf{n}}_r = 0, & \text{on } \Gamma_7, \end{cases} \quad (8)$$

where $\lambda_{ax(gl),left(right)}$ is the ion communication rate on the left (right) boundary of the axon (glial) compartment.

We use the Dirichlet boundary conditions for the perivascular space A & V boundary condition at location Γ_1 . For the pvsC and the ECS boundary condition, we use the homogeneous Neumann boundary condition at location Γ_1 . The membrane boundary conditions at locations $\Gamma_2 \cup \Gamma_6$ are used for the perivascular space A & V and the ECS. And the homogeneous Neumann boundary condition on $\Gamma_2 \cup \Gamma_6$ is used for the pvsC. The flux across the pia mater is assumed continuous and Ohm's law [7] and the additional pathway for diffusion, electric drift as well as convection for ions is used at location Γ_7 for the perivascular space A & C & V and the ECS.

$$\begin{cases} C_{pa}^i = C_{pa}^{i,re}, \quad C_{pv}^i = C_{pv}^{i,re}, \quad \nabla C_{pc}^i \cdot \hat{\mathbf{n}}_r = 0, \quad \nabla C_{ex}^i \cdot \hat{\mathbf{n}}_r = 0, & \text{on } \Gamma_1, \\ \nabla C_{pa}^i \cdot \hat{\mathbf{n}}_z = \lambda_{pa,left}(C_{pa}^i - C_{pa}^{i,re}), \quad \nabla C_{pv}^i \cdot \hat{\mathbf{n}}_z = \lambda_{pv,left}(C_{pv}^i - C_{pv}^{i,re}), & \text{on } \Gamma_2, \\ \nabla C_{ex}^i \cdot \hat{\mathbf{n}}_z = \lambda_{ex,left}(C_{ex}^i - C_{ex}^{i,re}), \quad \nabla C_{pc}^i \cdot \hat{\mathbf{n}}_z = 0, & \text{on } \Gamma_2, \\ \nabla C_{pa}^i \cdot \hat{\mathbf{n}}_z = \lambda_{pa,right}(C_{pa}^i - C_{pa}^{i,re}), \quad \nabla C_{pv}^i \cdot \hat{\mathbf{n}}_z = \lambda_{pv,right}(C_{pv}^i - C_{pv}^{i,re}), & \text{on } \Gamma_6, \\ \nabla C_{ex}^i \cdot \hat{\mathbf{n}}_z = \lambda_{ex,right}(C_{ex}^i - C_{ex}^{i,re}), \quad \nabla C_{pc}^i \cdot \hat{\mathbf{n}}_z = 0, & \text{on } \Gamma_6, \\ \mathbf{j}_{pa}^i \cdot \hat{\mathbf{n}}_r = \frac{G_{pia}^i}{z^i e} \left(\phi_{pa} - \phi_{csf} - \frac{k_B T}{e z^i} \log \left(\frac{C_{csf}^i}{C_{pa}^i} \right) \right) + C_{pa}^i u_{pa,csf}, & \text{on } \Gamma_7, \\ \mathbf{j}_{pv}^i \cdot \hat{\mathbf{n}}_r = \frac{G_{pia}^i}{z^i e} \left(\phi_{pv} - \phi_{csf} - \frac{k_B T}{e z^i} \log \left(\frac{C_{csf}^i}{C_{pv}^i} \right) \right) + C_{pv}^i u_{pv,csf}, & \text{on } \Gamma_7, \\ \mathbf{j}_{pc}^i \cdot \hat{\mathbf{n}}_r = \frac{G_{pia}^i}{z^i e} \left(\phi_{pc} - \phi_{csf} - \frac{k_B T}{e z^i} \log \left(\frac{C_{csf}^i}{C_{pc}^i} \right) \right), & \text{on } \Gamma_7, \\ \mathbf{j}_{ex}^i \cdot \hat{\mathbf{n}}_r = \frac{G_{pia}^i}{z^i e} \left(\phi_{ex} - \phi_{csf} - \frac{k_B T}{e z^i} \log \left(\frac{C_{csf}^i}{C_{ex}^i} \right) \right), & \text{on } \Gamma_7. \end{cases} \quad (9)$$

For the cerebrospinal fluid boundary, similar conditions are imposed except on Γ_5 , which a non-permeable boundary condition is used.

$$\begin{cases} C_{csf}^i = C_{csf}^{i,re}, & \text{on } \Gamma_3, \\ \nabla C_{csf}^i \cdot \hat{\mathbf{n}}_r = 0, & \text{on } \Gamma_4, \\ \mathbf{j}_{csf}^i \cdot \hat{\mathbf{n}}_z = 0, & \text{on } \Gamma_5, \\ \mathbf{j}_{csf}^i \cdot \hat{\mathbf{n}}_r = \sum_{l=pa,pv,pc,ex} \mathbf{j}_l^i \cdot \hat{\mathbf{n}}_r & \text{on } \Gamma_7. \end{cases} \quad (10)$$

1.2 Electric Potential

By multiplying equations 1 with $z_i e$ respectively, summing up, and using charge neutrality equation and ion flux equation, we have following system for the electric potential in ax, gl, ex, pa, pv, pc

$$\sum_i z^i e \left(\mathcal{M}_{ax,ex} J_{ax,ex}^i + \frac{\partial}{\partial z} (\eta_{ax} j_{ax,z}^i) \right) = 0, \quad (11a)$$

$$\sum_{k=ex,pa,pv,pc} \left(\sum_i z^i e (\mathcal{M}_{gl,k} J_{gl,k}^i) \right) + \sum_i z^i e (\nabla \cdot (\eta_{gl} \mathbf{j}_{gl}^i)) = 0, \quad (11b)$$

$$\sum_i z^i e (\mathcal{M}_{pa,ex} J_{pa,ex}^i - \mathcal{M}_{gl,pa} J_{gl,pa}^i + \mathcal{M}_{pa,pc} J_{pa,pc}^i + \nabla \cdot (\eta_{pa} \mathbf{j}_{pa}^i)) = 0, \quad (11c)$$

$$\sum_i z^i e (\mathcal{M}_{pv,ex} J_{pv,ex}^i - \mathcal{M}_{gl,pv} J_{gl,pv}^i - \mathcal{M}_{pc,pv} J_{pc,pv}^i + \nabla \cdot (\eta_{pv} \mathbf{j}_{pv}^i)) = 0, \quad (11d)$$

$$\sum_i z^i e (\mathcal{M}_{pc,ex} J_{pc,ex}^i - \mathcal{M}_{gl,pc} J_{gl,pc}^i - \mathcal{M}_{pa,pc} J_{pa,pc}^i + \mathcal{M}_{pc,pv} J_{pc,pv}^i + \nabla \cdot (\eta_{pc} \mathbf{j}_{pc}^i)) = 0, \quad (11e)$$

$$\sum_{k=ax,gl,pa,pv,pc} \left(- \sum_i z^i e (\mathcal{M}_{k,ex} J_{k,ex}^i) \right) + \sum_i z^i e (\nabla \cdot (\eta_{ex} \mathbf{j}_{ex}^i)) = 0, \quad (11f)$$

which describe the spatial distributions of electric potentials in six compartments.

In the subarachnoid space Ω_{SAS} , the governing equation for cerebrospinal fluid electric potential reduces to

$$\sum_i z^i e (\nabla \cdot \mathbf{j}_{csf}^i) = 0. \quad (12)$$

The boundary conditions for electric fields $\phi_{ax}, \phi_{gl}, \phi_{pa}, \phi_{pv}, \phi_{pc}, \phi_{ex}, \phi_{csf}$ are given below.

$$\left\{ \begin{array}{ll} \nabla \phi_l \cdot \hat{\mathbf{n}}_r = 0, \quad l = gl, pa, pv, pc, ex, & \text{on } \Gamma_1, \\ \nabla \phi_l \cdot \hat{\mathbf{n}}_z = 0, \quad l = ax, gl, pa, pv, pc, ex, & \text{on } \Gamma_2 \cup \Gamma_6, \\ \nabla \phi_{csf} \cdot \hat{\mathbf{n}}_r = 0, & \text{on } \Gamma_3 \cup \Gamma_5, \\ \nabla \phi_{csf} \cdot \hat{\mathbf{n}}_z = 0, & \text{on } \Gamma_4, \\ \nabla \phi_{gl} \cdot \hat{\mathbf{n}}_r = 0, & \text{on } \Gamma_7, \\ \sum_i z^i e \mathbf{j}_l^i \cdot \hat{\mathbf{n}}_r = \sum_i G_{pia}^i \left(\phi_l - \phi_{csf} - \frac{k_B T}{e z^i} \log \left(\frac{C_{csf}^i}{C_l^i} \right) \right), \quad l = pa, pv, pc, ex, & \text{on } \Gamma_7, \\ \sum_i z^i e \mathbf{j}_{csf}^i \cdot \hat{\mathbf{n}}_r = \sum_{l=pa,pv,pc,ex} \sum_i z^i e \mathbf{j}_l^i \cdot \hat{\mathbf{n}}_r & \text{on } \Gamma_7. \end{array} \right. \quad (13)$$

1.3 Fluid Circulation

In this subsection, we present the fluid circulation model. First, due to the conservation law, the volume fraction of each compartment $\eta_l, l = ax, gl, ex, pa, pv, pc$ satisfy

$$\frac{\partial \eta_{ax}}{\partial t} + \mathcal{M}_{ax,ex} U_{ax,ex} + \frac{\partial}{\partial z} (\eta_{ax} u_{ax}^z) = 0, \quad (14a)$$

$$\frac{\partial \eta_{gl}}{\partial t} + \mathcal{M}_{gl,ex} U_{gl,ex} + \mathcal{M}_{gl,pa} U_{gl,pa} + \mathcal{M}_{gl,pv} U_{gl,pv} + \mathcal{M}_{gl,pc} U_{gl,pc} + \nabla \cdot (\eta_{gl} \mathbf{u}_{gl}) = 0, \quad (14b)$$

$$\frac{\partial \eta_{pa}}{\partial t} + \mathcal{M}_{pa,ex} U_{pa,ex} - \mathcal{M}_{gl,pa} U_{gl,pa} + \mathcal{M}_{pa,pc} U_{pa,pc} + \nabla \cdot (\eta_{pa} \mathbf{u}_{pa}) = 0, \quad (14c)$$

$$\frac{\partial \eta_{pv}}{\partial t} + \mathcal{M}_{pv,ex} U_{pv,ex} - \mathcal{M}_{gl,pv} U_{gl,pv} - \mathcal{M}_{pc,pv} U_{pc,pv} + \nabla \cdot (\eta_{pv} \mathbf{u}_{pv}) = 0, \quad (14d)$$

$$\frac{\partial \eta_{pc}}{\partial t} + \mathcal{M}_{pc,ex} U_{pc,ex} - \mathcal{M}_{gl,pc} U_{gl,pc} - \mathcal{M}_{pa,pc} U_{pa,pc} + \mathcal{M}_{pc,pv} U_{pc,pv} + \nabla \cdot (\eta_{pc} \mathbf{u}_{pc}) = 0, \quad (14e)$$

$$\frac{\partial}{\partial z} (\eta_{ax} u_{ax}^z) + \sum_{k=gl,ex,pa,pv,pc} \nabla \cdot (\eta_k \mathbf{u}_k) = 0, \quad (14f)$$

$$\eta_{ax} + \eta_{gl} + \eta_{ex} + \eta_{pa} + \eta_{pv} + \eta_{pc} = 1, \quad (14g)$$

where $U_{l,k}$ is the fluid velocity across the membrane/interface between l_{th} and k_{th} compartments with surface volume ratio $\mathcal{M}_{l,k}$ and \mathbf{u}_l is the fluid velocity inside the l_{th} compartment.

The transmembrane fluid flux is proportional to the intracellular/extracellular hydrostatic pressure and osmotic pressure differences, i.e., Starling's law on the membrane, while the fluid flow from perivascular space A to perivascular space C and from perivascular space C to perivascular space V are only proportional to the difference of hydrostatic pressure due to the direct connection.

$$U_{l,ex} = L_{l,ex}(p_l - p_{ex} - \gamma_{l,ex}RT(O_l - O_{ex})), \quad l = ax, gl, pa, pv, pc \quad (15a)$$

$$U_{gl,l} = L_{gl,l}(p_{gl} - p_l - \gamma_{gl,l}RT(O_{gl} - O_l)), \quad l = pa, pv, pc. \quad (15b)$$

$$(15c)$$

Here $\gamma_{l,k}$ and $L_{l,k}$ are the reflection coefficient [8] and hydraulic permeability of the membrane between l_{th} and k_{th} compartments, respectively. In this paper osmotic pressure is defined by $RT O_l$ [7, 9]

$$O_l = \sum_i C_l^i + A_l \frac{\eta_l^{re}}{\eta_l}, \quad l = ax, gl,$$

$$O_l = \sum_i C_l^i, \quad l = ex, pa, pv, pc,$$

where $A_l \frac{\eta_l^{re}}{\eta_l} > 0$ is the density of the permanent negatively charged protein in glial cells and axons that varies with the volume (fraction) of the region, R is the molar gas constant, and T is temperature.

The hydrostatic pressure p_l and the volume fraction η_l are connected by the force balance on the membrane [9, 10]. The membrane force is balanced by the hydrostatic pressure difference on both sides of the semipermeable membrane. Then the variation of volume fraction from the resting state is proportional to the variation of hydrostatic pressure difference from the resting state.

$$K_l(\eta_l - \eta_l^{re}) = p_l - p_{ex} - (p_l^{re} - p_{ex}^{re}), \quad (16a)$$

where K_l is the stiffness constant and η_l^{re} and p_l^{re} are the resting state volume fraction and hydrostatic pressure of l_{th} compartment with $l = ax, gl, pa, pv, pc$.

The subarachnoid space region is modeled as a porous media filled with CSF. Therefore, the solution is incompressible in the Ω_{SAS} , and we have

$$\nabla \cdot \mathbf{u}_{csf} = 0, \quad in \ \Omega_{SAS}. \quad (17)$$

In the next section, we provide submodels of fluid velocities inside each compartment and the corresponding boundary conditions.

In this paper, we define a membrane boundary condition to describe the fluid or ion communication in the connect interface between the optic nerve and the retina or the optic canal or orbital. We assume this fluid or ion communication depend on the difference in pressure or ion concentration between the two sides of this connect interface $U_{int} = L(P_{in} - P_{out})$. Where U_{int} is the interface velocity, P_{in} and P_{out} are hydrostatic pressure on both sides of the interface, respectively.

Fluid Velocity in the Glial Compartment. The glial space is a connected space, where the intracellular fluid can flow from cell to cell through connexin proteins joining membranes of neighboring cells. The velocity of fluid in glial syncytium \mathbf{u}_{gl} depends on the gradients of hydrostatic pressure and osmotic pressure [7, 9, 10, 11, 12] as

$$u_{gl}^r = -\frac{\kappa_{gl}\tau_{gl}}{\mu} \left(\frac{\partial p_{gl}}{\partial r} - \gamma_{gl}RT \frac{\partial O_{gl}}{\partial r} \right), \quad (18a)$$

$$u_{gl}^\theta = -\frac{\kappa_{gl}\tau_{gl}}{\mu} \left(\frac{1}{r} \frac{\partial p_{gl}}{\partial \theta} - \gamma_{gl}RT \frac{1}{r} \frac{\partial O_{gl}}{\partial \theta} \right), \quad (18b)$$

$$u_{gl}^z = -\frac{\kappa_{gl}\tau_{gl}}{\mu} \left(\frac{\partial p_{gl}}{\partial z} - \gamma_{gl}RT \frac{\partial O_{gl}}{\partial z} \right), \quad (18c)$$

where κ_{gl} and τ_{gl} are the permeability and tortuosity of the glial compartment.

For the boundary condition, on the left and right boundaries of domain Ω_{OP} , the membrane boundary condition is used since they connect to intraocular and intracanalicular regions. On the top and bottom boundary, the no-flux boundary condition is used

$$\begin{cases} \mathbf{u}_{gl} \cdot \hat{\mathbf{n}}_r = 0, & \text{on } \Gamma_1 \\ \mathbf{u}_{gl} \cdot \hat{\mathbf{n}}_z = L_{gl,right}(p_{gl} - p_{gl,right}), & \text{on } \Gamma_2 \\ \mathbf{u}_{gl} \cdot \hat{\mathbf{n}}_z = L_{gl,left}(p_{gl} - p_{gl,left}), & \text{on } \Gamma_6 \\ \mathbf{u}_{gl} \cdot \hat{\mathbf{n}}_r = 0, & \text{on } \Gamma_7 \end{cases} \quad (19)$$

where $\hat{\mathbf{n}}_r$ and $\hat{\mathbf{n}}_z$ are the outward normal vector of domain Ω_p .

Fluid Velocity in the Axon Compartment. Since the axons are only connected in the longitudinal direction, the fluid velocity in the region of the axon is defined as

$$u_{ax}^r = 0, \quad (20a)$$

$$u_{ax}^\theta = 0, \quad (20b)$$

$$u_{ax}^z = -\frac{\kappa_{ax}}{\mu} \frac{\partial p_{ax}}{\partial z}, \quad (20c)$$

where κ_{ax} is the permeability of the axon compartment.

Similarly, membrane boundary conditions are used on the left and right boundaries

$$\begin{cases} \mathbf{u}_{ax} \cdot \hat{\mathbf{n}}_z = L_{ax,right}(p_{ax} - p_{ax,right}), & \text{on } \Gamma_2 \\ \mathbf{u}_{ax} \cdot \hat{\mathbf{n}}_z = L_{ax,left}(p_{ax} - p_{ax,left}), & \text{on } \Gamma_6 \end{cases} \quad (21)$$

Fluid Velocity in the Extracellular and Perivascular Spaces Since both the extracellular and perivascular spaces are narrow, the velocity is determined by the gradients of hydro-static pressure and electric potential [7, 13, 14], for $l = ex, pa, pv, pc$

$$u_l^r = -\frac{\kappa_l \tau_l}{\mu} \frac{\partial p_l}{\partial r} - k_e^l \tau_l \frac{\partial \phi_l}{\partial r}, \quad (22a)$$

$$u_l^\theta = -\frac{\kappa_l \tau_l}{\mu} \frac{1}{r} \frac{\partial p_l}{\partial \theta} - k_e^l \tau_l \frac{1}{r} \frac{\partial \phi_l}{\partial \theta}, \quad (22b)$$

$$u_l^z = -\frac{\kappa_l \tau_l}{\mu} \frac{\partial p_l}{\partial z} - k_e^l \tau_l \frac{\partial \phi_l}{\partial z}, \quad (22c)$$

where ϕ_l is the electric potential, τ_l is the tortuosity [15, 16], k_e^l describes the effect of electroosmotic flow [13, 14, 17], κ_l is the permeability.

For the boundary conditions, due to the connections to intraocular region and intracanalicular region on the left and right boundaries, respectively, membrane boundary conditions are used for extracellular and perivascular spaces A & V. Nonflux boundary condition is used for perivascular space c on Γ_2 and Γ_6 . On Γ_1 , due to the central blood vessels, Dirichlet boundary conditions on pressure are used for perivascular space A & V. For the ECS and pVSC, the zero penetration velocity is used. On the pia mater Γ_7 , the CSF could directly communicate with the perivascular spaces A & V due to the hydrostatic pressure difference. However, for ECS and pvsc, the CSF leaks into these two compartments through membranes. Then the velocity is fixed as the transmembrane velocity which depends on hydrostatic and osmotic pressure difference. In summary, the conditions are listed as follows

$$\begin{cases}
p_{pa} = p_{PA}, p_{pv} = p_{PV}, \mathbf{u}_{pc} \cdot \hat{\mathbf{n}}_r = 0, \mathbf{u}_{ex} \cdot \hat{\mathbf{n}}_r = 0, & \text{on } \Gamma_1 \\
\mathbf{u}_{pa} \cdot \hat{\mathbf{n}}_z = L_{pa,right}(p_{pa} - p_{pa,right}), \mathbf{u}_{pv} \cdot \hat{\mathbf{n}}_z = L_{pv,right}(p_{pv} - p_{pv,right}), & \text{on } \Gamma_2 \\
\mathbf{u}_{pc} \cdot \hat{\mathbf{n}}_z = 0, \mathbf{u}_{ex} \cdot \hat{\mathbf{n}}_z = L_{ex,right}(p_{ex} - p_{pv,right}), & \text{on } \Gamma_2 \\
\mathbf{u}_{pa} \cdot \hat{\mathbf{n}}_z = L_{pa,left}(p_{pa} - p_{pa,left}), \mathbf{u}_{pv} \cdot \hat{\mathbf{n}}_z = L_{pv,left}(p_{pv} - p_{IOP}), & \text{on } \Gamma_6 \\
\mathbf{u}_{pc} \cdot \hat{\mathbf{n}}_z = 0, \mathbf{u}_{ex} \cdot \hat{\mathbf{n}}_z = L_{ex,left}(p_{ex} - p_{IOP}), & \text{on } \Gamma_6 \\
\mathbf{u}_{pa} \cdot \hat{\mathbf{n}}_r = L_{pia,pa}(p_{pa} - p_{csf}), \mathbf{u}_{pv} \cdot \hat{\mathbf{n}}_r = L_{pia,pv}(p_{pv} - p_{csf}), & \text{on } \Gamma_7 \\
\mathbf{u}_{pc} \cdot \hat{\mathbf{n}}_r = L_{pia,pc}(p_{pc} - p_{csf} - \gamma_{pia}RT(O_{pc} - O_{csf})), & \text{on } \Gamma_7 \\
\mathbf{u}_{ex} \cdot \hat{\mathbf{n}}_r = L_{pia,ex}(p_{ex} - p_{csf} - \gamma_{pia}RT(O_{ex} - O_{csf})), & \text{on } \Gamma_7.
\end{cases} \quad (23)$$

where p_{IOP} is the intraocular pressure (IOP), γ_{pia} is the reflection coefficient of pia mater.

Fluid Velocity in the SAS Region. The cerebrospinal fluid velocity in the SAS region is determined by the gradients of hydro-static pressure and electric potential

$$u_{csf}^r = -\frac{\kappa_{csf}\tau_{csf}}{\mu} \frac{\partial p_{csf}}{\partial r} - k_e^{csf} \tau_{csf} \frac{\partial \phi_{csf}}{\partial r}, \quad (24a)$$

$$u_{csf}^\theta = -\frac{\kappa_{csf}\tau_{csf}}{\mu} \frac{1}{r} \frac{\partial p_{csf}}{\partial \theta} - k_e^{csf} \tau_{csf} \frac{1}{r} \frac{\partial \phi_{csf}}{\partial \theta}, \quad (24b)$$

$$u_{csf}^z = -\frac{\kappa_{csf}\tau_{csf}}{\mu} \frac{\partial p_{csf}}{\partial z} - k_e^{csf} \tau_{csf} \frac{\partial \phi_{csf}}{\partial z}, \quad (24c)$$

The fluid flow across the semi-permeable membrane Γ_4 is produced by the lymphatic drainage on the dura membrane, which depends on the difference between cerebrospinal fluid pressure and orbital pressure (OBP). At boundary Γ_3 , we assume the hydrostatic pressure is equal to the cerebrospinal fluid pressure. At boundary Γ_5 , a non-permeable boundary is used. On the pia membrane Γ_7 , the total CSF transmembrane velocity is determined by the conservation law,

$$\begin{cases}
p_{csf} = p_{CSF}, & \text{on } \Gamma_3 \\
\mathbf{u}_{csf} \cdot \hat{\mathbf{n}}_r = L_{dr}(p_{csf} - p_{OBP}), & \text{on } \Gamma_4 \\
\mathbf{u}_{csf} \cdot \hat{\mathbf{n}}_z = 0, & \text{on } \Gamma_5 \\
\mathbf{u}_{csf} \cdot \hat{\mathbf{n}}_r = L_{pia,ex}(p_{ex} - p_{csf} - \gamma_{pia}RT(O_{ex} - O_{csf})) \\
\quad + L_{pia,pa}(p_{pa} - p_{csf}) \\
\quad + L_{pia,pv}(p_{pv} - p_{csf}) \\
\quad + L_{pia,pc}(p_{pc} - p_{csf} - \gamma_{pia}RT(O_{pc} - O_{csf})), & \text{on } \Gamma_7
\end{cases} \quad (25)$$

where p_{CSF} is the cerebrospinal fluid pressure [18] in boundary Γ_3 .

2 Additional Tables and Figures

Table 1: Parameters in optic nerve model

Parameters	Value	Parameters	Value
R_a	$0.6 \times 10^{-5} m$ (**,Ref.[18, 19, 20])	μ	$7 \times 10^{-4} Pa \cdot s$ (Ref.[11])
R_b	$4.8 \times 10^{-5} m$ (Ref.[21, 6])	$C_{pa/pv/ex}^{Na,re}$	$111 mM$ (Ref.[18])
R_c	$6 \times 10^{-5} m$ (Ref.[5, 20])	$C_{pa/pv/ex}^{K,re}$	$4.5 mM$ (Ref.[18])
L	$1.5 \times 10^{-2} m$ (Ref.[21])	$C_{gl}^{Na,re}$	$5.72 mM$ (Ref.[5, 7])
e	$1.69 \times 10^{-19} A \cdot s$ (Ref.[21])	$C_{gl}^{K,re}$	$104.27 mM$ (*,Ref.[5, 18])
k_B	$1.38 \times 10^{-23} J/K$ (Ref.[21])	$C_{ax}^{Na,re}$	$7.33 mM$ (Ref.[5, 7])
T	$296.15 K$ (Ref.[21])	$C_{ax}^{K,re}$	$105.17 mM$ (Ref.[5, 7])
η_{ex}^{re}	1×10^{-1} (**,Ref.[21, 5])	$A_{ax,gl}^{re}$	$105 mM$ (Ref.[5, 7])
η_{ax}^{re}	4×10^{-1} (**,Ref.[21, 5])	K_{ax}	$1.67 \times 10^6 Pa$ (Ref.[22])
η_{gl}^{re}	4×10^{-1} (**,Ref.[21, 5])	K_{gl}	$8.33 \times 10^5 Pa$ (Ref.[22])
η_{pa}^{re}	2.4×10^{-2} (**,Ref.[21])	K_{pa}	$7.8 \times 10^6 Pa$ (*)
η_{pv}^{re}	6.39×10^{-2} (**,Ref.[21])	K_{pv}	$7.8 \times 10^6 Pa$ (*)
η_{pc}^{re}	1.21×10^{-2} (**,Ref.[21])	K_{pc}	$7.8 \times 10^6 Pa$ (*)
$\mathcal{M}_{ax,ex}$	$5.9 \times 10^6 m^{-1}$ (Ref.[23])	$L_{ax,ex}$	$7.954 \times 10^{-14} m/Pa \cdot s$ (Ref.[24])
$\mathcal{M}_{gl,ex}$	$6.25 \times 10^6 m^{-1}$ (Ref.[23])	$L_{gl,ex}$	$1.34 \times 10^{-13} m/Pa \cdot s$ (Ref.[7])
$\mathcal{M}_{gl,pa}$	$1.5 \times 10^6 m^{-1}$ (**,Ref.[23])	$L_{gl,pa/pc/pv}$	$1.34 \times 10^{-13} m/Pa \cdot s$ (**,Ref.[25, 26])
$\mathcal{M}_{gl,pv}$	$3.99 \times 10^6 m^{-1}$ (**,Ref.[23])	$L_{pa/pv,ex}$	$1 \times 10^{-15} m/Pa \cdot s$ (**,Ref.[25, 26])
$\mathcal{M}_{gl,pc}$	$7.56 \times 10^5 m^{-1}$ (**,Ref.[23])	$L_{pc,ex}$	$2.54 \times 10^{-15} m/Pa \cdot s$ (**,Ref.[25, 26])
$\mathcal{M}_{pa,ex}$	$1.21 \times 10^4 m^{-1}$ (**)	$L_{ax/gl/ax,left/right}$	$8.89 \times 10^{-12} m/Pa \cdot s$ (*,Ref.[5])
$\mathcal{M}_{pv,ex}$	$2.32 \times 10^4 m^{-1}$ (**)	$L_{pa,left/right}$	$3.32 \times 10^{-8} m/Pa \cdot s$ (*)
$\mathcal{M}_{pc,ex}$	$5.86 \times 10^4 m^{-1}$ (**)	$L_{pv,left}$	$1.37 \times 10^{-9} m/Pa \cdot s$ (*)
$z^{Na,K}$	1	$L_{pv,right}$	$6.64 \times 10^{-8} m/Pa \cdot s$ (*)
z^{Cl}	-1	$L_{pia,ex/pc/pv}$	$8.89 \times 10^{-13} m/Pa \cdot s$ (Ref.[5, 7])
$z^{ax,gl}$	-1 (Ref.[5])	$L_{pia,pa}$	$8.89 \times 10^{-13} m/Pa \cdot s$ (*,Ref.[5, 7])
γ	1 (Ref.[5, 11])	L_{dr}	$0 m/Pa \cdot s$ (**,Ref.[5, 7])
$K_{Na1,Na2}$	$2.3393 mM$ (Ref.[7])	τ_{gl}	0.5 (Ref.[5])
K_{K1}	$1.6154 mM$ (Ref.[7])	τ_{ex}	0.16 (Ref.[5, 11])
K_{K2}	$0.1657 mM$ (Ref.[7])	$\tau_{pa/pv/pc/csf}$	1 (**,Ref.[5])
$I_{gl,1}$	$4.78 \times 10^{-4} A/m^2$ (Ref.[7])	p_{CSF}	$2.1 \times 10^3 Pa$ (Ref.[5, 18])
$I_{gl,2}$	$6.5 \times 10^{-5} A/m^2$ (Ref.[7])	p_{OBP}	$0 \times 10^3 Pa$ (Ref.[5, 18])
$I_{ax,1}$	$9.56 \times 10^{-4} A/m^2$ (Ref.[7])	p_{IOP}	$4 \times 10^3 Pa$ (Ref.[5, 18])
$I_{ax,2}$	$1.3 \times 10^{-4} A/m^2$ (Ref.[7])	p_{AR}	$(1.5 \sim 1.485) \times 10^3 Pa$ (**,Ref.[5, 18])
$g_{gl/pa/pv/pc}^{Na}$	$2.2 \times 10^{-3} S/m^2$ (Ref.[5])	p_{VE}	$(0.5 \sim 0.475) \times 10^3 Pa$ (**,Ref.[5, 18])
$g_{gl/pa/pv/pc}^K$	$2.1 S/m^2$ (Ref.[5])	$p_{ax,left}$	$-12 \times 10^3 Pa$ (**)
$g_{gl/pa/pv/pc}^{Cl}$	$2.2 \times 10^{-3} S/m^2$ (Ref.[5])	$p_{ax,right}$	$-14 \times 10^3 Pa$ (**)
g_{leak}^{Na}	$4.8 \times 10^{-3} S/m^2$ (Ref.[5])	$p_{gl,left}$	$-24 \times 10^3 Pa$ (**)
g_{leak}^K	$2.2 \times 10^{-2} S/m^2$ (Ref.[5])	$p_{gl,right}$	$-27 \times 10^3 Pa$ (**)
\bar{g}^{Na}	$13.57 S/m^2$ (Ref.[5])	$p_{ex,right}$	$0.4 \times 10^3 Pa$ (**)
\bar{g}^K	$2.945 S/m^2$ (Ref.[5])	$p_{pv,right}$	$0.4 \times 10^3 Pa$ (**)
g_{ax}^{Cl}	$1.5 \times 10^{-1} S/m^2$ (Ref.[5])	$p_{pa,left}$	$1.4 \times 10^3 Pa$ (**)
$G_{pia}^{Na,K,Cl}$	$3 S/m^2$ (Ref.[5])	$p_{pa,right}$	$1.6 \times 10^3 Pa$ (**)
$k_e^{ex/pa/pv/pc}$	$1.3729 \times 10^{-8} m^2/V \cdot s$ (**,Ref.[5])	$D_{ex/ax/pa/pv/pc}^{Na}$	$1.39 \times 10^{-9} m^2/s$ (**,Ref.[5])
k_e^{csf}	$0 m^2/V \cdot s$ (**,Ref.[5])	$D_{ex/ax/pa/pv/pc}^K$	$2.04 \times 10^{-9} m^2/s$ (**,Ref.[5])
κ_{ax}	$1.33 \times 10^{-16} m^2$ (Ref.[5, 11])	$D_{ex/ax/pa/pv/pc}^{Cl}$	$2.12 \times 10^{-9} m^2/s$ (**,Ref.[5])
κ_{ex}	$3.99 \times 10^{-16} m^2$ (Ref.[5, 11])	D_{gl}^{Na}	$1.39 \times 10^{-11} m^2/s$ (Ref.[5, 11])
$\kappa_{pa/pv}$	$2 \times 10^{-12} m^2$ (**,Ref.[26, 25])	D_{gl}^K	$2.04 \times 10^{-11} m^2/s$ (Ref.[5, 11])
κ_{gl}	$9.366 \times 10^{-19} m^2$ (Ref.[5, 11])	D_{gl}^{Cl}	$2.12 \times 10^{-11} m^2/s$ (Ref.[5, 11])
κ_{csf}	$1.33 \times 10^{-14} m^2$ (Ref.[5, 11])	$\lambda_{ax/ex/gl/pa/pv,left}$	$20 m^{-1}$ (*)
κ_{pc}	$2 \times 10^{-19} m^2$ (**,Ref.[26, 25])	$\lambda_{ax/ex/gl/pa/pv,right}$	$20 m^{-1}$ (*)

Note: the '*', estimated or induced from the concentration balance.

Note: the '**', estimated or deducted proportional from reference.

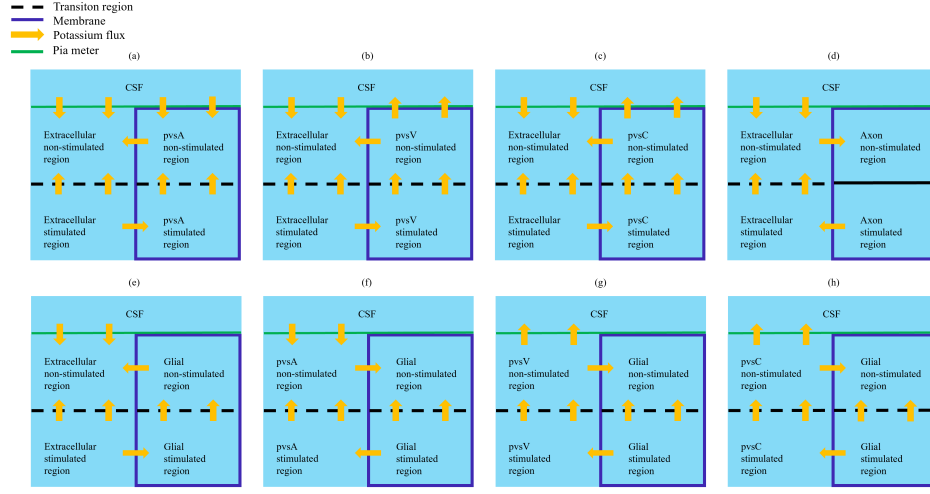


Figure 1: Schematic graph of the potassium microcirculation between two compartments when inner part axon was stimulated. (a) Extracellular-pvsA; (b) Extracellular-pvsV; (c) Extracellular-pvsC; (d) Extracellular-Axon; (e) Extracellular-Glial; (f) Glial-pvsA; (g) Glial-pvsV; (h) Glial-pvsC; The dash black line is the interface between stimulus region and unstimulus region. The solid black line in axon compartment means the potassium flux only in z direction and can not transition between the stimulated and non-stimulated region.

References

- [1] Lori A Ray, Martin Pike, Matthew Simon, Jeffrey J Iliff, and Jeffrey J Heys. Quantitative analysis of macroscopic solute transport in the murine brain. *Fluids and Barriers of the CNS*, 18:1–19, 2021.
- [2] Richard Fitzhugh. Thresholds and plateaus in the hodgkin-huxley nerve equations. *The Journal of general physiology*, 43(5):867–896, 1960.
- [3] Fabrizio Gabbiani and Steven James Cox. Mathematics for neuroscientists. *Academic Press*, 2017.
- [4] Junyuan Gao, X Sun, V Yatsula, RS Wymore, and RT Mathias. Isoform-specific function and distribution of na/k pumps in the frog lens epithelium. *The Journal of membrane biology*, 178(2):89–101, 2000.
- [5] Yi Zhu, Shixin Xu, Robert S Eisenberg, and Huaxiong Huang. A tridomain model for potassium clearance in optic nerve of necturus. *Biophysical journal*, 120(15):3008–3027, 2021.
- [6] H. Bracho, P. Orkand, and R. Orkand. A further study of the fine structure and membrane properties of neuroglia in the optic nerve of necturus. *Journal of neurobiology*, 6(4):395–410, 1975.
- [7] Yi Zhu, Shixin Xu, Robert Eisenberg, and Huaxiong Huang. A bidomain model for lens microcirculation. *Biophysical journal*, 116(6):1171–1184, 2019.
- [8] Joseph J Feher. *Quantitative Human Physiology: An Introduction*. Academic press, 2017.
- [9] Shixin Xu, Bob Eisenberg, Zilong Song, and Huaxiong Huang. Osmosis through a semi-permeable membrane: a consistent approach to interactions. *arXiv preprint arXiv*, 1806.00646, 2018.
- [10] Mori Yoichiro. A multidomain model for ionic electrodiffusion and osmosis with an application to cortical spreading depression. *Physica D Nonlinear Phenomena*, 308:94–108, 2015.
- [11] R T Mathias. Steady-state voltages, ion fluxes, and volume regulation in syncytial tissues. *Biophysical Journal*, 48(3):435–448, 1985.

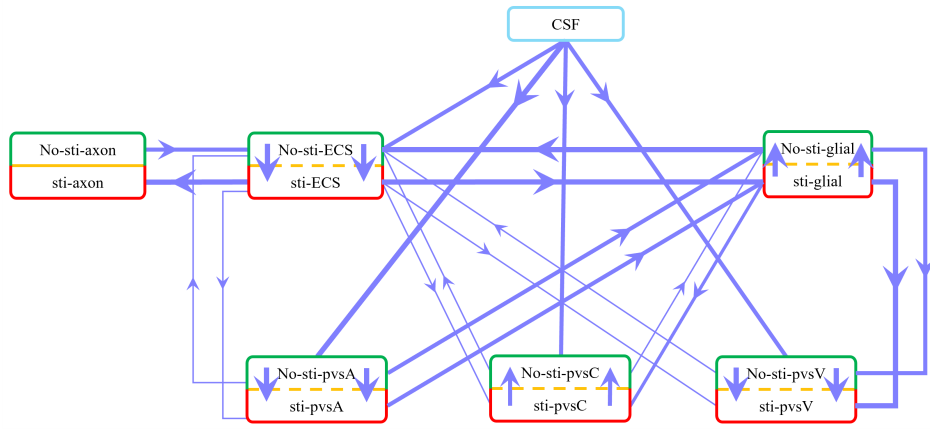


Figure 2: Schematic of fluid flux between the stimulated (lower) and non-stimulated (upper) regions, as well as transmembrane fluid flux between different compartments during stimulation. Red boxes represent the stimulated regions, and green boxes represent the non-stimulated regions. The thickest lines indicate fluxes around 10^{-3} /s, moderately thick lines represent fluxes around 10^{-4} /s, and the thinnest lines indicate fluxes less than 10^{-5} /s. The transmembrane fluid flux is MU .

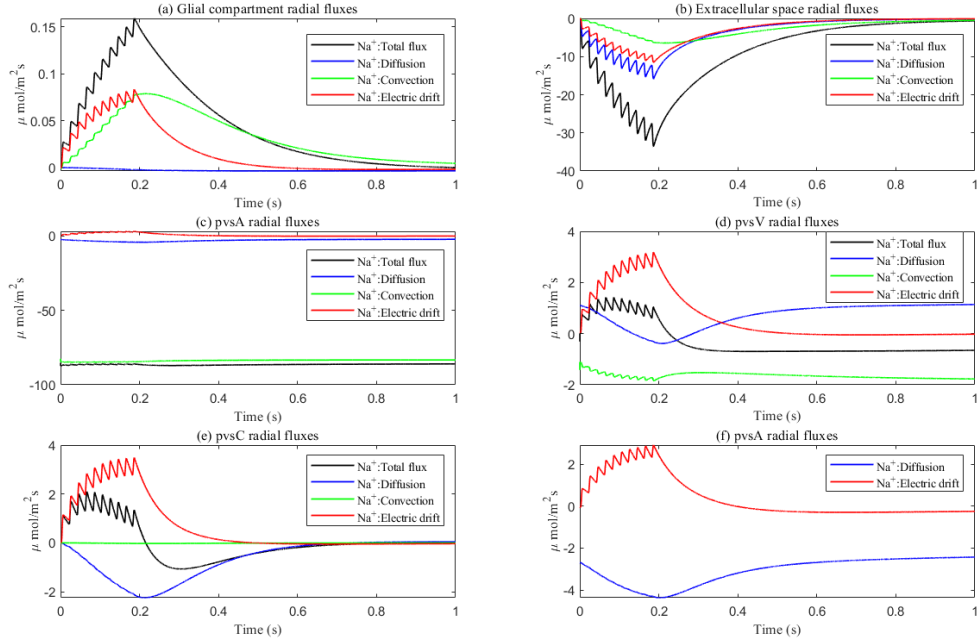


Figure 3: Average radial direction Na^+ fluxes components in the intradomain. The Na^+ fluxes in (a) Glial compartment; (b) ECS; (c) pvs A; (d) pvs V; (e) pvs C; (f) zoom in of diffusion and electric drift flux in pvs A.

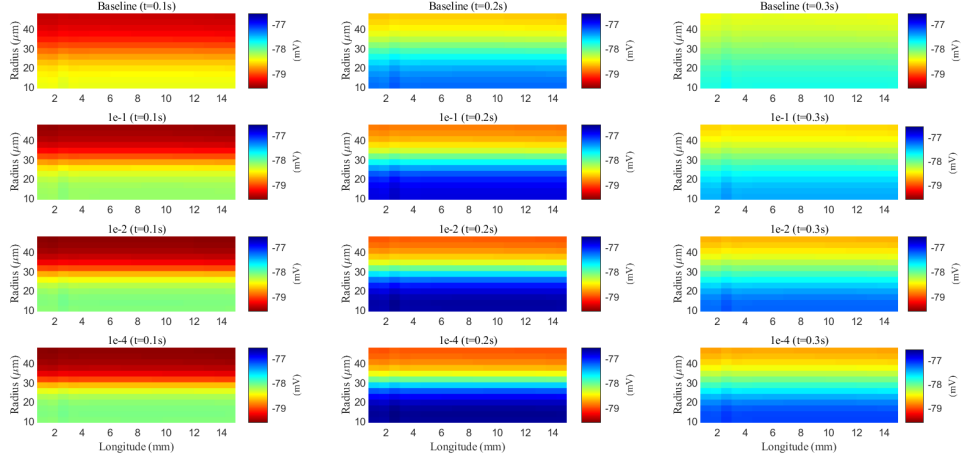


Figure 4: Spatial distribution of membrane potential during and after a train of stimuli in the glial compartment. Different rows are results with different connectivity of glial compartment; Different columns are results at different time slots.

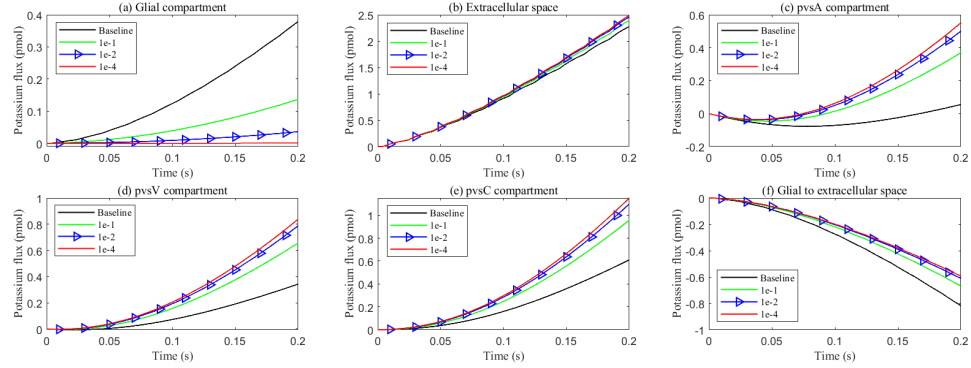


Figure 5: Cumulative potassium fluxes during the stimulus with varying levels of glial connexin connectivity. a-e: Radial cumulative potassium fluxes within compartments. f: Cumulative transmembrane potassium fluxes in the stimulated region.

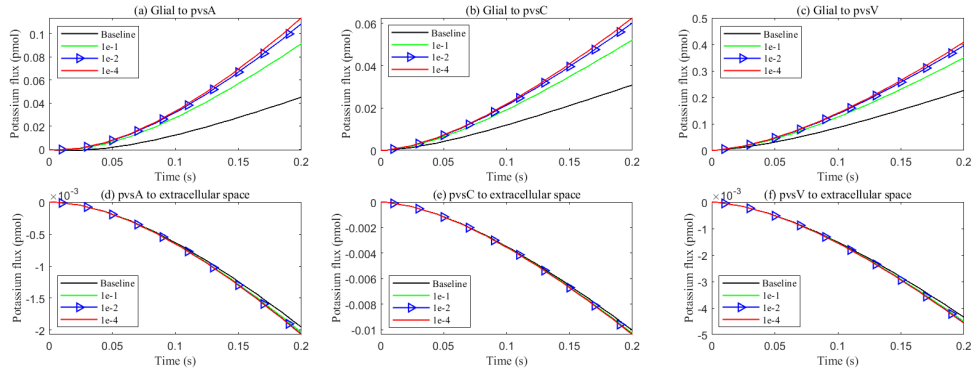


Figure 6: Cumulative transmembrane potassium fluxes in the stimulated region during the stimulus with varying levels of glial connexin connectivity. (a) Glial to pvs A; (b) Glial to pvs C; (c) Glial to pvs V; (d) pvs A to ECS; (E) pvs C to ECS; (F) pvs V to ECS.

- [12] R.T. Mathias, J.L. Rae, and R.S. Eisenberg. Electrical properties of structural components of the crystalline lens. *Biophysical Journal*, 25(1):181–201, 1979.
- [13] Li Wan, Shixin Xu, Maijia Liao, Chun Liu, and Ping Sheng. Self-consistent approach to global charge neutrality in electrokinetics: A surface potential trap model. *Physical Review X*, 4(1):011042, 2014.
- [14] Ehsan Vaghefi, Duane T K Malcolm, Marc D Jacobs, and Paul J Donaldson. Development of a 3d finite element model of lens microcirculation. *BioMedical Engineering OnLine*, 11,1(2012-09-19), 11(1):69, 2012.
- [15] Charles Nicholson. Diffusion and related transport mechanisms in brain tissue. *Reports on Progress in Physics*, 64(7):815, 2001.
- [16] MA Pérez-Pinzón, LIAN Tao, and CHARLES Nicholson. Extracellular potassium, volume fraction, and tortuosity in rat hippocampal ca1, ca3, and cortical slices during ischemia. *Journal of Neurophysiology*, 74(2):565–573, 1995.
- [17] STUART McLAUGHLIN and RICHARD T Mathias. Electro-osmosis and the reabsorption of fluid in renal proximal tubules. *The Journal of general physiology*, 85(5):699–728, 1985.
- [18] Leah R Band, Cameron L Hall, Giles Richardson, and andAlexanderJE Foss Oliver EJensen, JenniferHSiggers. Intracellular flow in optic nerve axons: A mechanism for cell death in glaucoma. *Investigative Ophthalmology & Visual Science*, 50(8):3750–3758, 2009.
- [19] Eytan Raz, Maksim Shapiro, Timothy M. Shepherd, Erez Nossek, Shadi Yaghi, Doria M. Gold, Koto Ishida, Janet C. Rucker, Irina Belinsky, Eleanore Kim, Brian Mac Grory, Osman Mir, Mari Hagiwara, Shashank Agarwal, Matthew G. Young, Steven L. Galetta, and Peter Kim Nelson. Central retinal artery visualization with cone-beam ct angiography. *Radiology*, 302(2):419–424, 2022.
- [20] Ning Wang. Intraocular and intracranial pressure gradient in glaucoma. *Springer*, 1, 2019.
- [21] SW Kuffler, JG Nicholls, and RK Orkand. Physiological properties of glial cells in the central nervous system of amphibia. *Journal of Neurophysiology*, 29(4):768–787, 1966.
- [22] William H Morgan, Chandrakumar Balaratnasingam, Christopher R P Lind, Steve Colley, Min H Kang, Philip H House, and Dao Yi Yu. Cerebrospinal fluid pressure and the eye. *British Journal of Ophthalmology*, 100(1):71–77, 2016.
- [23] Ch. Pilgrim, I. Reisert, and D. Grab. Volume densities and specific surfaces of neuronal and glial tissue elements in the rat supraoptic nucleus. *Journal of Comparative Neurology*, 211(4):427–431, 1982.
- [24] R. Villegas and G. M. Villegas. Characterization of the membranes in the giant nerve fiber of the squid. *The Journal of general physiology*, 43(5):73, 1960.
- [25] Ravi Teja Kedarasetti, Patrick J. Drew, and Francesco Costanzo. Arterial vasodilation drives convective fluid flow in the brain: a poroelastic model. *Fluids and Barriers of the CNS*, 19(34), 2022.
- [26] Marie E. Rognes et al. Lars Willas Dreyer, Anders Eklund. Modeling csf circulation and the glymphatic system during infusion using subject specific intracranial pressures and brain geometries. *Fluids and Barriers of the CNS*, 1, 2024.